Ring opening of decalin and methylcyclohexane over alumina-based monofunctional WO₃/Al₂O₃ and Ir/Al₂O₃ catalysts

Rodrigo Moraes [a], Karine Thomas [a], Sébastien Thomas [a], Sander Van Donk [b], Giacomo Grasso [b], Jean-Pierre Gilson [a], Marwan Houalla [a,*]

[a] Laboratoire Catalyse et Spectrochimie, ENSICAEN – Université de Caen – CNRS, 6 Bd. du Maréchal Juin, 14050 Caen, France
[b] Total Petrochemicals Research S.A., Zone industrielle CB-7181, Feluy, Belgium

ARTICLE INFO

ABSTRACT

Ring-opening reactions of decalin and MCH were studied over monofunctional acid (WO₃/Al₂O₃) and metal (Ir/Al₂O₃) catalysts containing, respectively, up to 5.3 at. W/nm² and 1.8 wt% Ir. The catalysts were characterized by X-ray diffraction, Raman spectroscopy, low-temperature CO adsorption followed by infrared spectroscopy, and H₂ chemisorption. A reaction network was proposed for both molecules and used to determine the kinetic parameters. Kinetic modeling allowed relating characterization results and catalytic performance. For WO₃/Al₂O₃ catalysts, ring contraction precedes ring opening of both molecules. The evolution of ring contraction activity was consistent with the development of relatively strong Brønsted acid sites. Ring opening occurs according to a classic acid mechanism. For Ir/Al₂O₃ catalysts, only direct ring opening was observed. Ring opening proceeds mostly via dicarbene mechanism. Analysis of products indicated that monofunctional metal catalysts are better suited than acid solids for upgrading LCO.

1. Introduction

In order to meet an increasing demand for diesel, especially in Europe, oil refiners have the option to blend some of the Light Cycle Oil (LCO) fraction, produced in the Fluid Catalytic Cracking (FCC) process, with the diesel pool. However, with the exception of the carbon number, the LCO does not meet current diesel specifications, especially in Europe. It contains high amounts of polyaromatics (*ca.* 48–69%) and low cetane number (*ca.* 18–25) when compared to the European norms (polyaromatics: upper limit of 11% – cetane number: minimum of 51). Hence, the LCO must be deeply hydrotreated. The polycyclic aromatic fraction can be lowered by hydrogenation, which also improves the cetane index. However, this increase is not sufficient, and a ring opening of naphthenic compounds appears to be required for LCO to significantly contribute to the diesel pool. As illustrated in Table 1, the cetane number significantly increases when a molecule such as decalin with two naphthenic rings is converted into linear or monobranched paraffins. Ring opening must, thus, be highly selective toward these products. Naphthene ring opening can be achieved over metal, acid and bifunctional catalysts. One of the simplest mononaphthenic molecule, and as a consequence the most studied, is methylcyclohexane (MCH). This model molecule consists of a six-
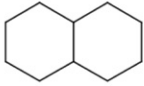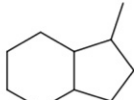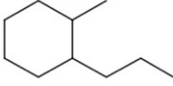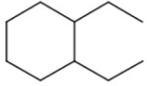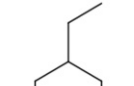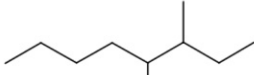
carbon atom ring with one alkyl ramification. This limits the number of possible reaction products and facilitates the establishment of a reaction network. As a result, hydroconversion of MCH and other similar single-ring naphthenes has been the subject of many studies [1–24]. However, MCH cannot be considered as representative of the LCO mixture, and thus, its use as a probe molecule to study the LCO upgrading reaction can be questioned. The LCO product distribution shows that it consists mainly of two-ring aromatic systems [25], making two-ring naphthenes such as decalin, in hydrotreated feeds, a logical choice as probe molecules for the study of LCO upgrading. In contrast to studies involving mono C₄, C₅, and C₆ naphthenic rings, literature concerning selective ring opening of model molecules containing two fused rings for LCO upgrading, such as decalin, tetralin, or naphthalene, is more limited [16,26–35]. The study of such molecules is very often hindered by the analytical difficulties, due to the complexity of ring opening and other concomitant reactions (e.g., isomerization and cracking). Detailed identification of the intermediates and products obtained in these reactions is required for a better understanding of the mechanism of ring opening reaction and an appropriate selection of the most suitable catalytic system [36].

Acid-catalyzed ring opening of naphthenes has been mainly studied on zeolites [3–5,19,28,29,33,37,38]. The majority of these studies involve single-ring molecules [3–5,19,37,38]. Recently, several studies have attempted to gain insight into the acid-catalyzed ring opening of decalin [28,29,33]. Kubicka et al. [28] and

Table 1
Cetane number of some relevant decalin ring-opening products [35].

Santikunaporn et al. [29] showed that decalin ring opening over zeo-lites is preceded by ring contraction (e.g., isomerization from a cyclohexyl to a cyclopentyl ring). Kubicka et al. [28] also reported that Brønsted acidity influences the ring-opening yield. The best performance was obtained for catalysts with moderate Brønsted acidity (Hβ-25, Hβ-75 and HY-12 zeolites) with, virtually, no activity observed for catalysts with low Brønsted acidity (MCM-41) and fast deactivation due to coke deposits with solids exhibiting strong Brønsted acid sites (H-mordenite-20). It is believed that ring open-ing of naphthenes over acid catalysts proceeds on Brønsted acid sites and is initiated by protolytic dehydrogenation followed by chain reactions of the carbenium ions formed (e.g., ring contraction, β-scission, alkylations and hydride transfer) [4,28,33].

McVicker et al. [16] investigated selective ring opening of naph-thenic molecules over several metals (Ru, Rh, Ni, Ir and Pt). It was observed that Ru, Rh and Ni exhibit similar preference for cleaving unsubstituted C–C bonds, but are generally less selective than Ir. Pt is much less active but can break substituted C–C bonds, leading to an approximately statistical product distribution [8]. Paál et al. [39] reported that metals such as Rh, Pd, Ir and Pt promote single hydrogenolysis of 3-methylpentane and methylcyclohexane, whereas multiple fragmentation (i.e., leading to the formation of compounds with less than 7 carbon atoms) was observed for Co, Ni, Cu, Ru, Ag, Re and Os. Overall, the literature shows that irid-ium-based catalysts exhibit high activity and selectivity for ring opening of C_5 and C_6 monocyclic molecules [13,16,40].

With respect to ring opening mechanism over metal catalysts, Gault [8] reported that hydrogenolysis of substituted naphthenes can take place over Pt/Al$_2$O$_3$ according to three distinct mechanisms: (1) non-selective mechanism (occurring on highly dispersed plati-num) corresponding to an equal chance of breaking any C–C bond of the ring (multiplet mechanism); (2) selective mechanism allow-ing only the rupture of unsubstituted C–C bonds (dicarbene mecha-nism); and (3) a "partially selective" mechanism, competing with the dicarbene mechanism (on poorly dispersed Pt catalysts), involv-ing metallocyclobutane species as an intermediate (metallocyclob-utane mechanism). In recent studies, the metallocyclobutane mechanism has been frequently invoked to interpret results, involv-ing the cleavage of methyl-substituted C–C bonds that could not be explained by the multiplet or the dicarbene mechanisms [6,16,41].

In addition to the behavior of monofunctional metal and acid catalysts, it was observed that C_6 ring-opening reaction of naphth-enes is enhanced by the use of bifunctional catalysts [2,13,16,21,26,29,32,42–46]. This has been interpreted by C_6 to C_5 ring contraction over the acid function and a greater ease of opening C_5 rings over the metal function [16,42,43].

Zirconia was proved to be an attractive support for bifunctional catalysts because of the possibility of fine tuning its acidity by con-trolled tungsten deposition [47]. We have recently shown that by using tungstated zirconia as supports, after Ir deposition, high per-formance bifunctional Ir–W catalysts for selective ring opening of methylcyclohexane can be developed [13,45]. However, zirconia is not a typical industrial support and lacks the textural and mechanical properties of more conventional supports such as alu-mina. Moreover, the shaped industrial catalyst for such a reaction will be produced by extrusion, and alumina is the binder of choice for such a process. Thus, it was of interest to develop an alternative alumina-supported system and compare its performance with the corresponding zirconia-based system. The results showed that identical performance (products distribution, and selectivity) for MCH ring opening can be obtained when alumina is used as a sup-port instead of zirconia [48].

The present work extends previous studies of MCH ring opening over alumina-based catalysts to decalin, a molecule that is more representative of the LCO cut. It involves a detailed investigation of the performance of WO$_x$-based monofunctional acid catalysts and Ir-based monofunctional metal catalysts for decalin conver-sion. Specifically, it includes a systematic study of the effect of W surface density (WO$_3$/Al$_2$O$_3$) and iridium loading (Ir/Al$_2$O$_3$) on the structure of the catalysts and on their activity and selectivity for decalin ring-opening reaction and a comparison of the results with those obtained for MCH reaction. A reaction network is proposed for both naphthenes and a kinetic model is developed to fit the reactivity results, thus enabling the investigation of structure-cat-alytic performance relationship. Finally, potential improvement of the cetane number will be evaluated based on the nature and com-position of decalin ring-opened products. The present work will serve as a basis for future study aimed at achieving a better under-standing of the behavior of bifunctional catalysts.

2. Experimental

2.1. Materials

The γ-Al$_2$O$_3$ support (AX 300) was supplied by Criterion. It exhibited, after calcination at 773 K for 2 h, a specific surface area

of 256 m^2 g^{-1} and a pore volume of 0.69 cm^3 g^{-1}. The W phase (4–32 wt% W) was deposited by impregnation of the support with ammonium metatungstate solution followed by calcination at 1023 K for 3 h. The W loadings used correspond to surface densities ranging from 0.5 to 5.3 at. W/nm^2. The latter were calculated assuming that the surface area is only due to the alumina. Tungstated alumina catalysts were designated as AWx where x is the W surface density expressed as atoms W/nm^2. The series of yIr/AW0 (y = 0.6, 1.2 and 1.8 wt.%) catalysts was prepared by incipient wetness impregnation with a 50 g/l hydrogen hexachloroiridate (IV) hexahydrate solution (Acros Organics) followed by drying at 393 K for 12 h and calcination at 723 K for 3 h with a (20% v/v O_2 with N_2 as carrier) flow of 25 ml min^{-1}.

2.2. BET surface area

The specific surface area of the catalyst was determined from physical adsorption of N_2 at T = 77 K, by applying the BET equation on the part of the adsorption isotherm with $0.05 \leqslant p/p° \leqslant 0.35$. The adsorption isotherms were measured with a Micromeritics ASAP 2000 apparatus. The samples were first outgassed at 573 K in a dynamic vacuum for 1 h.

2.3. X-ray diffraction

Powder X-ray diffraction patterns were recorded with a Philips X'pert diffractometer (PW1750 spectrometer), using the Cu Kα radiation. The angle (2θ) was varied from 20° to 80° in 0.02° steps. The crystalline structure of the phases present was identified by comparison with the database of the Joint Committee on Powder Diffraction Standards (JCPDS).

2.4. Raman spectroscopy

Raman studies were carried out under ambient conditions using samples in a powder form. The Raman spectrometer consisted of a confocal microscope Labram 300 (Jobin Yvon), equipped with a Nd/YAG laser (frequency doubled, 532 nm) and a CCD detector. The power on the sample was about 13 mW.

2.5. Infrared spectroscopy

The infrared spectra were recorded at low temperature with a Nicolet Nexus FTIR spectrometer equipped with a MCT detector. The powder was pressed into a self-supported wafer (∼15 mg). The activation of the wafer was carried out in situ in a flow infrared cell under dry air at 673 K for 2 h, followed by treatment under H_2 for 1 h at 623 K. The sample was then cooled to 473 K, evacuated under vacuum for 2 h, and cooled to room temperature. The infrared cell was then evacuated for 1 h and cooled to 100 K. The infrared spectra were acquired following introduction of increments of CO and finally in the presence of 133 Pa of CO at equilibrium. All spectra were normalized to 15 mg of the solid.

2.6. H_2 chemisorption measurements

Hydrogen chemisorption measurements were obtained with an in house apparatus using a TCD detector. The samples were previously pre-treated at 573 K for 1 h, under 5 MPa of hydrogen, in order to duplicate the conditions of the catalytic tests. Before the measurements, the sample (300 mg) was reduced in flowing hydrogen (50 cm^3 min^{-1}) at 573 K for 1 h, purged in ultra pure Ar (50 cm^3 min^{-1}) for 1 h, and then cooled down to room temperature. The metallic function was characterized by two series of H_2 micropulses. After activation of the catalyst, pulses of H_2 were injected at room temperature every minute up to saturation. The

consumed amount observed was attributed to chemisorbed and physisorbed hydrogen. After 10 min of purging under pure Ar, a new series of pulses were injected over the sample, to determine the reversible part of the adsorbed hydrogen. The irreversible fraction (chemisorbed H_2) was taken as the difference between the two values. Dispersion data were obtained assuming a H/surface Ir stoichiometry of adsorption of 1. The stoichiometry of H/Ir = 1 adopted in the present study for Ir dispersions lower than 60% was based on previous results for the same system where the Ir particle size estimated from H_2 chemisorption was compared with that obtained by TEM measurements [49,50].

2.7. Methylcyclohexane ring opening

Methylcyclohexane (MCH) ring opening was carried out at a total pressure of 5 MPa, for a temperature range of 523–623 K and for contact times between 10 and 20 g h mol^{-1}, in a continuous flow fixed-bed microreactor containing 1 g of catalyst, diluted in 1 g of silicon carbide. The partial pressures of hydrogen and MCH were set at 4.8 and 0.2 MPa, respectively. MCH was dried over activated 3A zeolite and delivered through a liquid chromatography pump (Gilson 302). Before testing, each catalyst was activated in situ under atmospheric pressure at 673 K with flowing dry air for 2 h and cooled to 623 K under flowing dry He. The sample was then treated at 623 K in a dry hydrogen flow for 1 h and then cooled to 573 K prior to increasing the pressure. Hydrogen (Air Liquide, Grade I) and helium (Air Liquide, Grade U) gases were further purified from water and oxygen contaminants with 3A zeolite and BTS (FLUKA) traps. The product gas mixture was collected at atmospheric pressure and analyzed online with a Varian 3400 gas chromatograph equipped with a flame ionization detector and a Chrompack CP-SIL 5 CB WCOT fused silica capillary column.

The products analysis, attribution, and calculation of MCH conversion are described elsewhere [13].

A wide range of MCH conversion was obtained by varying the contact time and the reaction temperature.

2.8. Decalin ring opening

Decalin ring opening was carried out at a total pressure of 5 MPa, in a temperature range of 523–623 K and at contact times between 170 and 320 g h mol^{-1}, in a continuous flow fixed-bed microreactor containing 1 g of catalyst, diluted in 1 g of silicon carbide. The feed, consisting of a mixture of 89% (v/v) n-heptane and 11% (v/v) decalin, (cis/trans molar ratio of 40:60), was delivered through a liquid chromatography pump (Gilson 302). The mixture decalin/n-heptane was dried over activated 3A zeolite. The partial pressure of hydrogen, n-heptane, and decalin were set at 4.874, 0.113, and 0.013 MPa, respectively. The product gas mixture was collected at atmospheric pressure and analyzed online with a Varian 3800 gas chromatograph, fitted with a capillary column (HP-PONA, length 50 m, internal diameter 0.2 mm) and a flame ionization detector (FID) detector. Before the activity test, each catalyst was activated in situ at atmospheric pressure at 673 K with flowing dry air for 2 h, cooled to 623 K under dry He flow. As noted for the methylcyclohexane reaction, the sample was treated at 623 K in a dry hydrogen flow for 1 h and then cooled to 573 K prior to increasing the pressure. Hydrogen (Air Liquide, Grade I) and helium (Air Liquide, Grade U) gases were further purified from water and oxygen contaminants with 3A zeolite and BTS (FLUKA) traps.

Decalin conversion leads to a complex mixture of about 250 compounds. The products were identified by GC–MS, GC × GC-TOFMS at Total Petrochemicals Research Centers. GC–MS analyses were performed using a HP-PONA column identical to that mentioned above. The GC × GC-TOFMS method used as primary column a HP-5MS (non-polar, 30 m, internal diameter 0.32 mm, film

thickness 0.25 μm), and as secondary column a SolGelWax (polar, 1.5 m, internal diameter 0.10 mm, film thickness 0.20 μm).

To facilitate the evaluation of the results, the products were grouped. All the alkyl-substituted monocyclic C10 were referred to as one-ring-opening products (1ROP); linear or branched C10 were denoted two-ring-opening products (2ROP); bicyclical C10 where one or both rings consist of less than 6 carbon atoms were named ring contraction products (RCP); compounds with lower molecular weight than that of decalin were denoted as cracking products (CP). Under some experimental conditions (high temperatures, active catalysts), the *n*-heptane solvent in the decalin feed can react and form isomers and cracking products. This was taken into consideration in estimating decalin conversion and products yield.

Decalin conversion was varied by changing the contact time and the reaction temperature.

3. Results

3.1. Monofunctional acid catalysts

3.1.1. Texture and composition of the AWx solids

The BET surface area, corrected surface area of the Al_2O_3 support (assuming that the surface area is only due to the alumina support), W loading (determined by ICP) and the corresponding W surface density (at. W/nm^2), over the WO_x/Al_2O_3 catalysts, are listed in Table 2. As shown in Table 2, the corrected surface area remains essentially constant in the W surface density range examined. The surface area of the alumina support was lower than that of the tungstated solids, reflecting the stabilization effect of the W phase.

3.1.2. X-ray diffraction (XRD)

The XRD patterns of the AWx solids for various W surface densities are shown in Fig. 1. All solids exhibit the main reflections lines of the gamma alumina support ($2\theta = 37.6°$, $45.8°$ and $66.7°$). In addition, the main lines characteristic of WO_3 ($2\theta = 23.1°$, $23.6°$, $24.2°$, $33.6°$ and $34.0°$) were detected for W surface densities $\geqslant 4.1$ at. W/nm^2. A weak and an ill-defined band, at $2\theta = 23.1–24.2°$ which can be attributed to the most intense lines of WO_3, was also evidenced for the AW2.9 solid. This suggests that up to 4.1 at. W/nm^2, the tungsten phase is essentially present in the form of a surface phase.

3.1.3. Raman spectroscopy

The Raman spectra of the AWx samples under ambient conditions are shown in Fig. 2. For all W surface densities, the catalysts exhibit a Raman band at 952–976 cm^{-1} which was assigned to W surface interaction species [51–53]. Raman bands due to WO_3 crystalline particles ($\sim$808, 717 and 273 cm^{-1}) were observed for W surface densities $\geqslant 2.9$ at. W/nm^2.

Table 2
Texture and composition of the AWx solids.

Sample	W loading (wt.%)	S_{BET} ($m^2\,g^{-1}$)	$S_{corrected}$[a] ($m^2\,g^{-1}$)	W surface density (at. W/nm^2)
AW0	–	222	222	0
AW0.5	3.8	230	243	0.5
AW1.4	9.4	220	249	1.4
AW2.9	18.9	201	263	2.9
AW4.1	24.0	182	256	4.1
AW5.3	28.5	158	246	5.3

[a] $S_{corrected} = \frac{S_{measured}}{1 - \frac{W\,(wt.\%)}{100} \cdot 1.216}$.
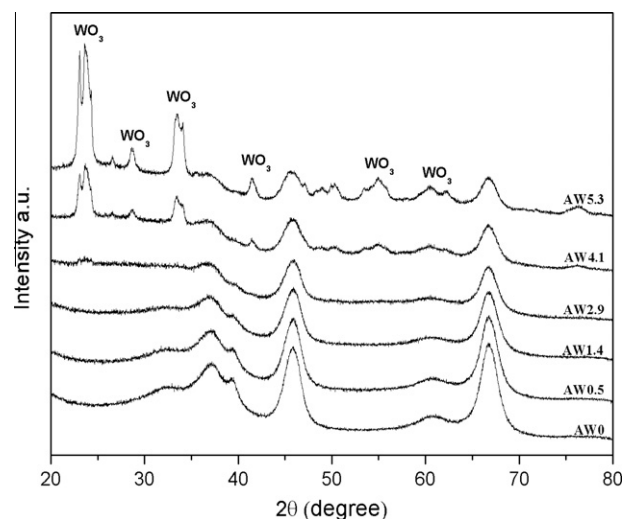

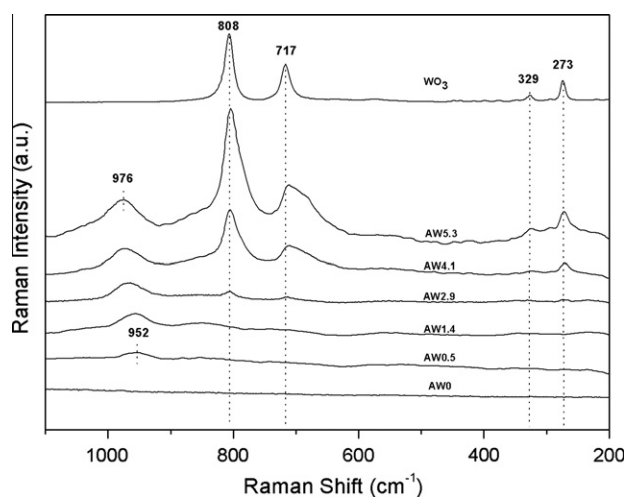**Fig. 1.** X-ray diffraction patterns for the tungstated alumina catalysts (AWx).

Fig. 2. Raman spectra of the AWx catalysts under ambient conditions.

3.1.4. Low-temperature CO adsorption monitored by infrared spectroscopy

Several probe molecules, including carbon monoxide, pyridine and lutidine, can be used to characterize the acidity of oxide surfaces. Low-temperature CO adsorption monitored by infrared spectroscopy, adopted in the present study, offers the advantage of being sensitive to the strength of Brønsted acid sites thus titrated [54,55]. The interaction between CO and the hydroxyl groups leads to a shift to lower wavenumbers of the $v(OH)$ vibration and a shift to higher wavenumbers of the (CO) vibration. The position of (CO) vibration is thus characteristic of the strength of the acid site probed [54,56,57].

After activation, changes in the infrared spectra of different catalysts were observed in the OH region (not shown). The intensity of the area associated with the OH stretching region decreased gradually with increasing W surface density. This was attributed to a progressive replacement of the OH groups by W species [58,59]. Similar phenomena have been observed for other metal oxides supported on alumina [60,61].

Infrared spectra, following introduction of small increments of CO, were acquired to facilitate the detection of strong acid sites which may be present in minor amounts, since these sites will react first. Fig. 3 shows the infrared spectra for the AWx series in the
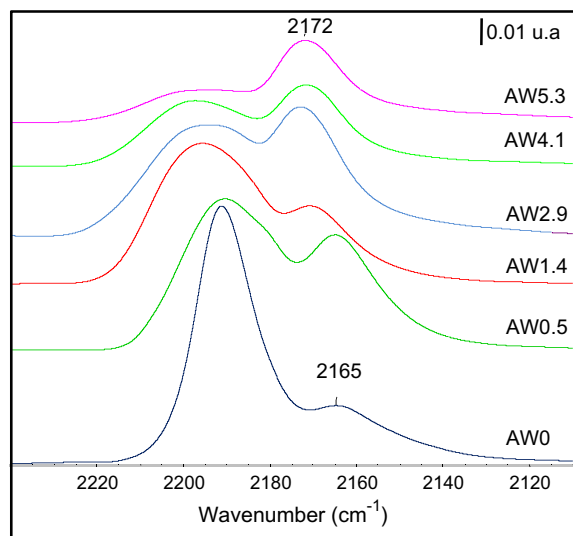
Fig. 3. Infrared spectra in the v(CO) region for AWx series after introduction of 3.5 μmol CO following subtraction of the spectrum of the activated catalysts.

(CO) region after introduction of 3.5 μmol of CO and subtraction of the spectrum of activated catalysts. The band located in the 2180–2220 cm^{-1} region is attributed to CO coordinated to Al^{3+} sites [62] and that at 2165–2172 cm^{-1} is ascribed to Brønsted acid sites [63]. For W surface density $\geqslant 2.9$, the latter band is centered at $ca.$ 2172–2173 cm^{-1}, indicating the presence of relatively strong Brønsted acid sites [63]. The development of these sites was associated with the formation of polymeric W surface species.

Fig. 4a shows the infrared spectra in the v(CO) region obtained after the introduction of 133 Pa CO. For the alumina support, CO adsorption at 100 K gives rise to a strong band at 2155 cm^{-1} assigned to CO weakly bonded to OH groups and a shoulder at 2143 cm^{-1} ascribed to physisorbed CO on the alumina surface. With increasing W surface density, the position of v(CO) band, associated with CO interaction with Brønsted acid sites, shifts upward from 2155 for AW0 catalysts to 2162 cm^{-1} for AW2.9 catalysts. This shift was accompanied by a strong decrease in

intensity and can be attributed to a preferential consumption of the most basic OH groups with initial tungsten deposition. For W surface density $\geqslant 2.9$ at. W/nm^2, as seen in Fig. 3, a new band at higher frequency appears (2172 cm^{-1}) and the position of v(CO) increases up to 2166 cm^{-1} for AW5.3 catalyst.

The evolution of Brønsted and Lewis acid sites with W surface density was then determined using the infrared spectra of the catalysts following the introduction of 133 Pa of CO at equilibrium in the 2060–2240 cm^{-1} region. The decomposition of the envelope was carried out according to the parameters determined in a previous work [63].

Fig. 4b shows an example of the decomposition of the envelope for the solid AW4.1. The spectra were curve fitted using 7 Gaussian bands: The three bands located in the 2180–2205 cm^{-1} region were assigned to Lewis acid sites. The band at 2172 cm^{-1} was attributed to relatively strong Brønsted acid sites and that at 2155–2164 cm^{-1} was ascribed to weak Brønsted acid sites. The band at 2143 cm^{-1} and the shoulder at 2130–2132 cm^{-1} are associated with physisorbed CO. The variation of the normalized area of the bands attributed to Brønsted and Lewis acid sites (Fig. 5a and b) reflects the evolution of the abundance of the corresponding acid sites. A decrease in the abundance of Lewis acid sites and weak Brønsted acid sites with increasing W surface density is observed (Fig. 5a). This was attributed to an increased coverage of the alumina support on W deposition [63,64]. In contrast, a different evolution of relatively strong Brønsted acid sites was observed (Fig. 5b). It can be clearly seen that for W surface density lower than 1.4 at. W/nm^2, no strong Brønsted acid sites (band at 2172 cm^{-1}) were detected. For W surface density >1.4 at. W/nm^2, the abundance of the strong Brønsted acid sites increased almost linearly with increasing W surface density.

3.1.5. Decalin and MCH conversion: influence of W surface density
3.1.5.1. Activity. Fig. 6 shows the evolution of the composition of cis- and trans-isomers in the unconverted decalin as a function of conversion for the AW4.1 catalyst. The results indicate that the cis/trans ratio gradually decreases with increasing conversion. This is consistent with the results reported by Lai et al. [65], in the case of HY zeolites, and may simply reflect the higher reactivity of the cis form [29,66].
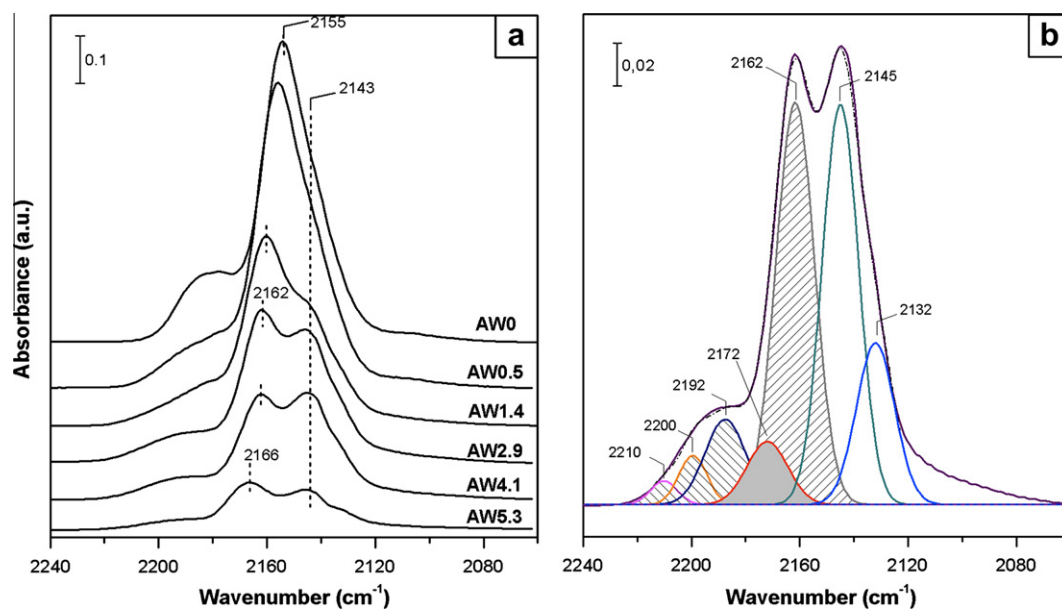

Fig. 4. Infrared spectra of the v(CO) region for the (a) series of AWx catalysts with different W surface density after the introduction of 133 Pa CO at equilibrium and following subtraction of the spectrum of the activated catalysts and (b) curve fitting results for the AW4.1 catalyst. Solid line, experimental spectrum; dotted line, reconstituted spectrum after curve fitting.
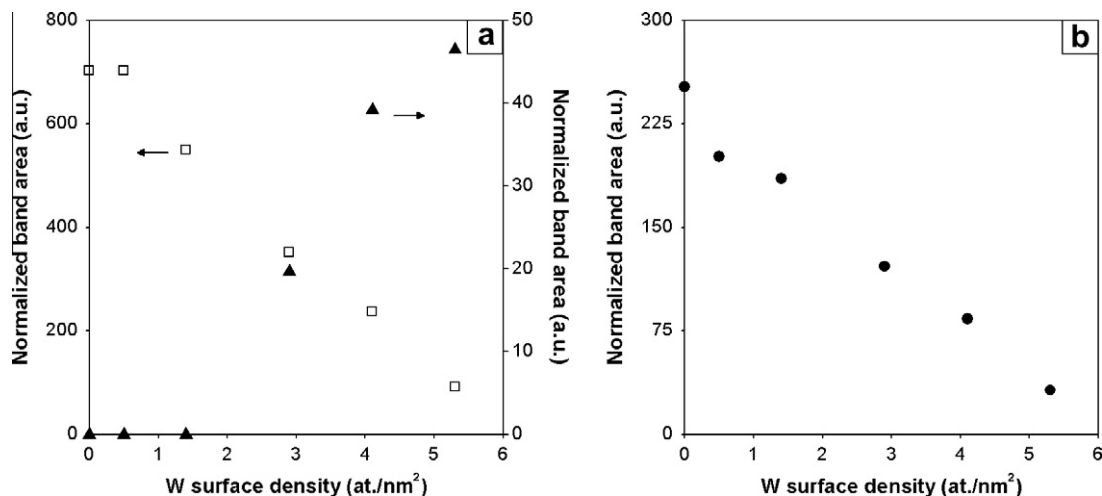
Fig. 5. Evolution of the abundance of acid sites for tungsten alumina catalysts (AWx) after introduction of 133 Pa CO at equilibrium at 100 K: (a) relatively strong Brønsted acid sites (▲); weak Brønsted acid sites (■); and (b) Lewis sites (●).
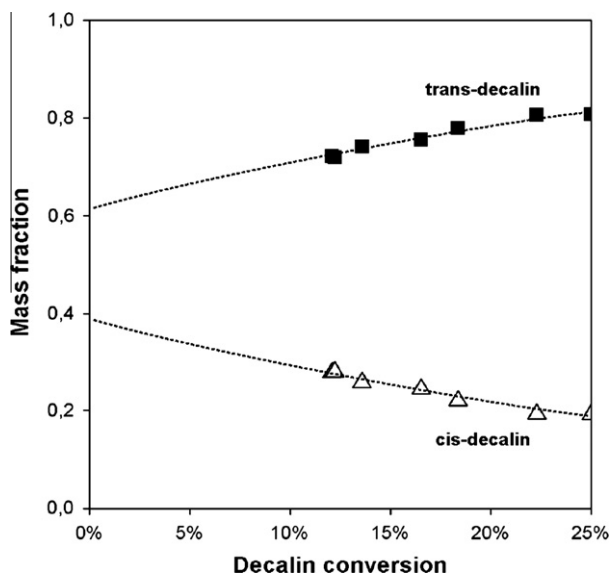

Fig. 6. Cis- and trans-decalin internal composition as a function of conversion for the AW4.1 catalyst.

Fig. 7 shows the variation of decalin and MCH conversion for the AWx catalysts as a function of W surface density, for a reaction temperature of 623 K and a contact time of 20 g h mol^{-1}. The results for decalin were obtained by extrapolation of the conversion obtained at a higher contact time assuming first order kinetics. Similar conversions were observed for both naphthenes. No significant activity was observed for W surface densities lower or equal to 1.4 at. W/nm^2. For higher W surface densities, the conversion increased with increasing W surface density up to 4.1 at. W/nm^2 and leveled off for the AW5.3 solid. The activity observed for these catalysts appears to be associated with the formation of relatively strong Brønsted acid sites for W surface densities higher than 1.4 at. W/nm^2. A similar behavior was reported by Lecarpentier et al. [13] for MCH conversion over WO_3/ZrO_2–SiO_2.

3.1.5.2. Selectivity. The performance of the catalysts, for decalin and MCH ring opening, was monitored. The evolution of ring opening, ring contraction, and cracking products selectivities with conversion for the three active catalysts is shown in Fig. 8. The results clearly show that, for both reactions at a given conversion, the three active catalysts exhibit similar selectivities. This suggests that the active sites are associated with Brønsted acid sites of similar strengths present in these solids.
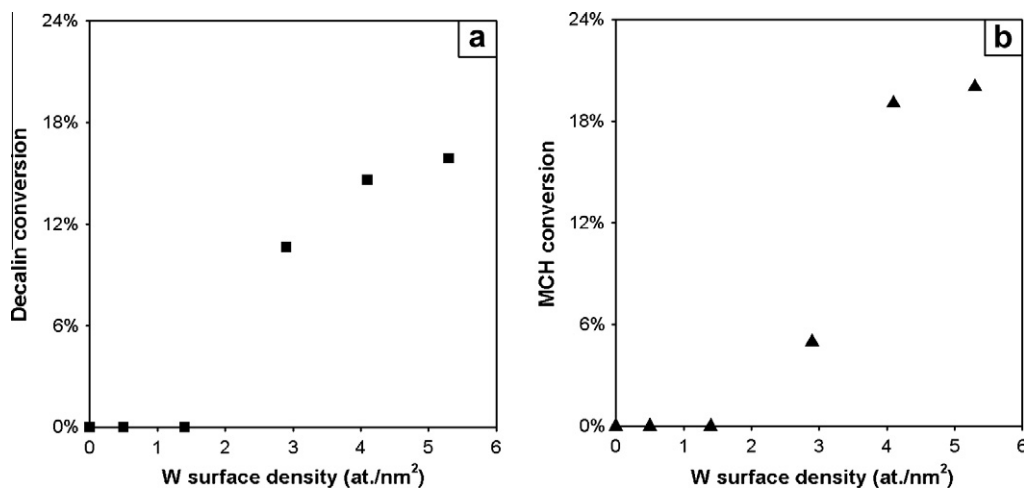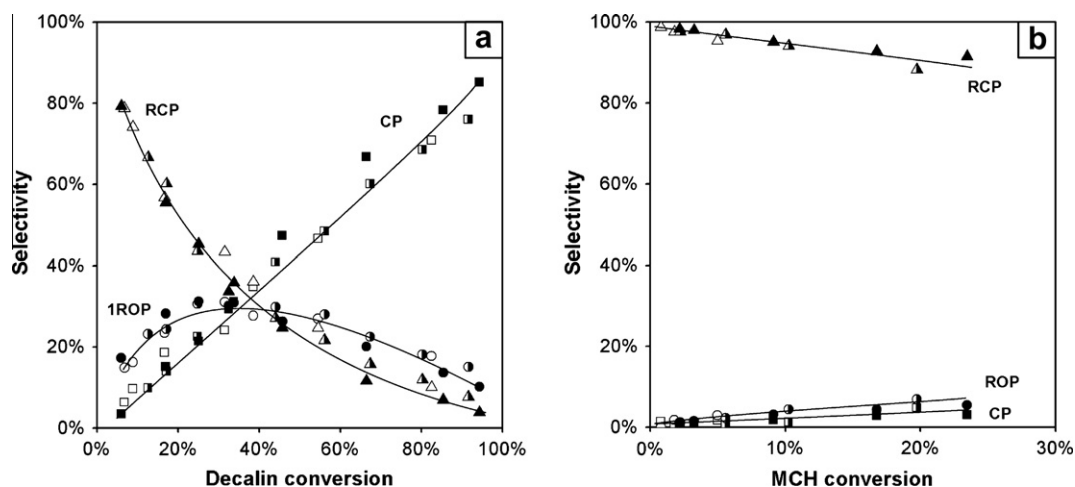

Fig. 7. (a) Decalin and (b) MCH conversion obtained with the AWx catalysts as a function of the W surface density at 623 K and a contact time of 20 g h mol^{-1}.

Fig. 8. Product selectivities obtained with the AWx catalysts as a function of: (a) decalin and (b) MCH conversion (open symbols: $x = 2.9$; half-filled symbols: $x = 4.1$; and filled symbols: $x = 5.3$).

For low conversions, the selectivity for RCP tends to *ca.* 100%, whereas those for 1ROP and CP tend to *ca.* 0% with decreasing conversion. This indicates that cracking and ring opening of both naphthenic molecules are preceded by ring contraction. The secondary nature of the ring opening products has also been reported by Kubicka et al. [28] and Santikunaporn et al. [29] for decalin over zeolites and by Lecarpentier et al. [13] for the conversion of methylcyclohexane over WO$_3$/ZrO$_2$–SiO$_2$ catalysts. The observed decrease in RCP selectivity with increasing conversion can be attributed to the cracking and ring opening of ring-contracted products. At low conversion, the major cracking products of decalin were isobutane and C$_6$ (namely methylcyclopentane), as reported by Kubicka et al. [28] and Santikunaporn et al. [29]. This suggests that the cracking of 1ROP (butylcycloalkane intermediate) to form isobutane and a methylcycloalkane is favored over that of RCP (methyl-substituted binaphthene [36]), yielding typically by cracking C$_1$ and C$_9$ products.

The high CP selectivity observed at high conversion of decalin can be attributed to the cracking of RCP and 1ROP. Note that only a small amount of 2ROP (not shown) was detected (up to 2% of selectivity) at high conversion. This is consistent with the reported difficulty in breaking endocyclic C–C bonds compared to exocyclic ones [67,68] during hydrocracking of C$_{10}$ naphthenes.

As shown for decalin, RCP selectivity for the MCH reaction (Fig. 8b) also tends to 100% at low conversion and decreases with increasing conversion. However, the decrease in selectivity is less pronounced for the MCH reaction, suggesting that the RCP formed during the MCH reaction are less reactive than those of decalin. Furthermore, a much lower CP selectivity was observed for the MCH reaction when compared to that of decalin.

For both reactions, traces of aromatics (e.g., toluene and tetralin) and olefins were observed. This is consistent with previous studies of the ring opening of naphthenic molecules over acid catalysts [28,29,69].

Fig. 9a depicts the evolution of the molar selectivities of C$_{10}$H$_{20}$ ROPs within the one-ring opening group of products, obtained for the three active AWx catalysts, as a function of decalin conversion. Analysis of the 1ROPs internal distribution shows that ethyl-dimethylcyclohexanes (EDMCH) are the most abundant compounds. For simplification purposes, less abundant products with three or more alkyl substituents, such as tetramethylcyclohexanes and dimethyl-propylcyclopentanes, were grouped and identified as "Others". Lower amounts of methyl-propylcyclohexanes (MPCH), butylcyclohexanes (BCH), pentylcyclopentanes (C5CP), and "Others" were detected. It should be noted that under the examined conditions, iso-butylcyclohexane accounts for over 80% of the BCH group of product.

Fig. 9b depicts the evolution of the molar selectivities of C$_7$H$_{14}$ ROP within the ring opening group of products, obtained for the three active AWx catalysts, as a function of MCH conversion.
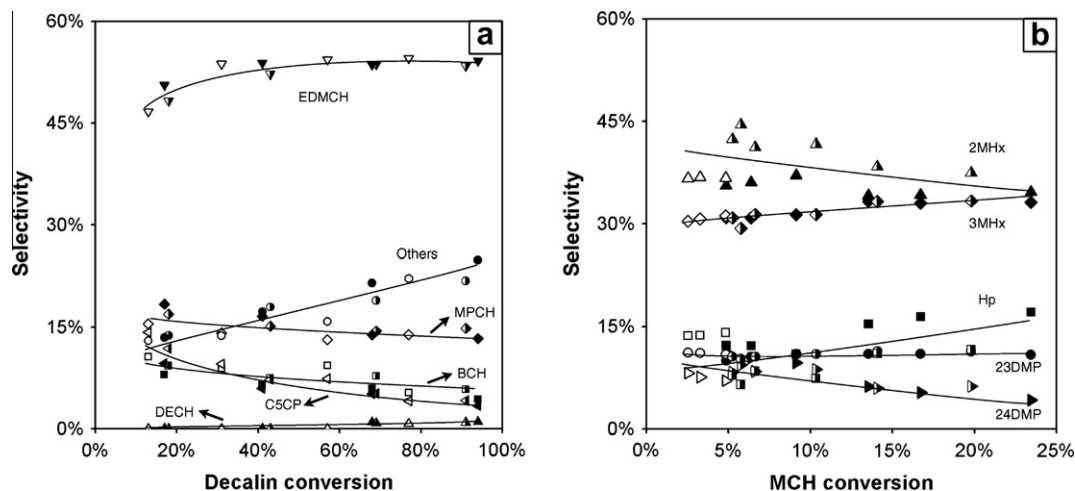

Fig. 9. Molar selectivities of: (a) C$_{10}$H$_{20}$ 1ROPs and (b) C$_7$H$_{14}$ ROPs, within the one-ring opening group of products, obtained with the AWx catalysts, as a function of the corresponding naphthene conversion (open symbols: $x = 2.9$; half-filled symbols: $x = 4.1$; and filled symbols: $x = 5.3$).
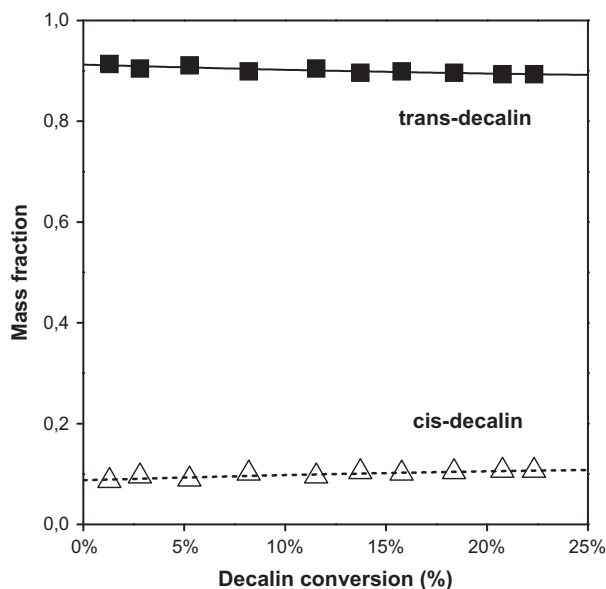
Fig. 10. Cis- and trans-decalin internal composition as a function of conversion for the yIr/AW0 catalysts.

Analysis of the internal distribution of ROP, for the MCH reaction, shows that methylhexanes (2MHx and 3MHx) are the most abundant compounds followed by dimethylpentanes (23DMP and 24DMP) and heptane (Hp) in comparable amounts. No trimethylbutanes or ethylpentanes were detected. The results in Fig. 9a and b show that for the three active catalysts, at a given conversion, essentially the same product selectivity was obtained.

3.2. Monofunctional metal catalysts

3.2.1. H_2 chemisorption measurements

A series of Ir/Al$_2$O$_3$ catalysts (noted yIr/AW0) containing up to 1.8 wt% Ir were prepared. Dispersion values of 56, 46, and 40% were obtained for the catalysts containing 0.6, 1.2, and 1.8 wt%, respectively.

3.2.2. Decalin and MCH conversion: influence of Ir content
3.2.2.1. Activity. Fig. 10 depicts the evolution of the internal composition of cis- and trans-isomers as a function of conversion for the yIr/AW0 catalyst. The results show that for very low decalin con-

version, the cis/trans ratio is very close to the thermodynamic equilibrium composition (ca. 10:90). This suggests that, in contrast to what was observed for the W monofunctional acid catalysts, the cis–trans equilibrium is rapidly reached over Ir metal catalysts. Similar observations were reported by Lai et al. [65] when comparing proton-form and Pt or Pd loaded zeolites and where ascribed to metal-catalyzed dehydrogenation/hydrogenation reactions.

Fig. 11 shows the variation of decalin conversion for the yIr/AW0 catalysts as a function of Ir loading for a reaction temperature of 623 K and a contact time of 20 g h mol^{-1}. As reported for the monofunctional acid catalysts, decalin conversion was extrapolated to a contact time of 20 g h mol^{-1}, assuming first order kinetics. The results show that conversion, for both decalin and MCH, increases with iridium content. For these catalysts, increasing iridium content brings about a slight decrease in the dispersion (55–40%). As a result, the overall number of available surface metal sites increases with iridium content. Hence, the observed increase in conversion reflects the increase in the number of surface metal sites. It is also observed that under the same conditions, for a given Ir loading, MCH conversion is higher than that of decalin. Higher reactivity of MCH as compared to decalin can be inferred from the work of McVicker et al. [16]. As noted previously, over these catalysts, the cis/trans thermodynamic equilibrium composition (10–90 vs. 40–60 in the starting decalin) is rapidly reached, resulting in the enrichment of the reactant mixture in trans-decalin. Trans-decalin is reportedly less reactive than cis-decalin [29,66], which was attributed, for the acid-catalyzed reaction, to a more hindered tertiary C–H bond, in trans-decalin, making protonation and formation of adsorbed carbocations more difficult than in the case of cis-decalin. In the present case, a lower reactivity of the trans form is consistent with its lower ring strain as compared with the cis-form (ca. −7.9 kJ mol^{-1} vs. 5.0 kJ mol^{-1}, respectively [70]). In addition, trans-decalin exhibits lower ring strain than that of MCH (ca. 4.2 kJ mol^{-1} [16]). Thus, one can tentatively attribute the lower activity of decalin to the higher stability of trans-decalin when compared to that of MCH. It should be noted, however, that because of the use of n-heptane as a solvent in the decalin feed, one cannot rule out possible inhibition of decalin conversion because of competitive adsorption of n-heptane.

3.2.2.2. Selectivity. The performance of the monofunctional metal catalysts, for decalin ring opening, was monitored and compared with that of MCH. Fig. 12 reports the selectivities for 1ROP, CP, and 2ROP, for all the monofunctional metal catalysts, as a function of decalin and MCH conversion. The results show that, for a given
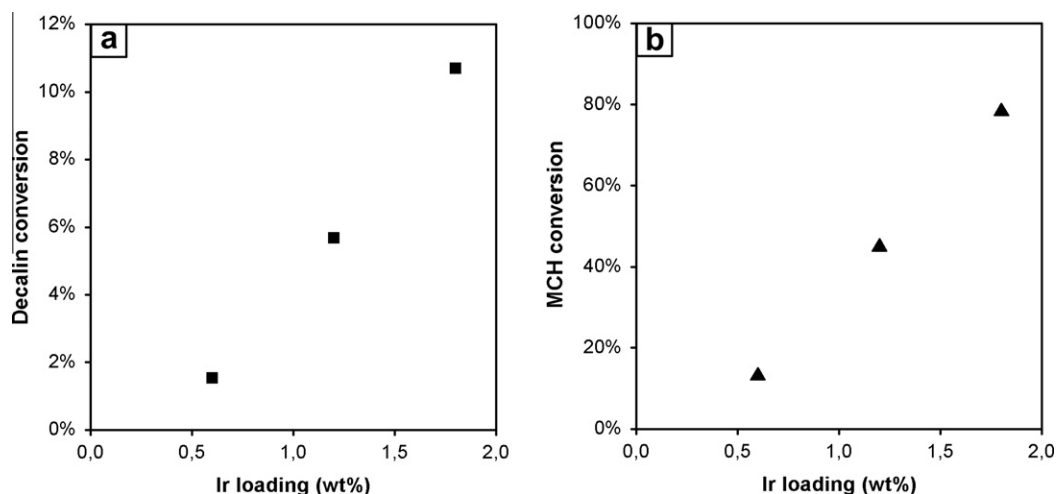

Fig. 11. (a) Decalin and (b) MCH conversion obtained with the yIr/AW0 catalysts as a function of the Ir loading at 623 K and a contact time of 20 g h mol^{-1}.
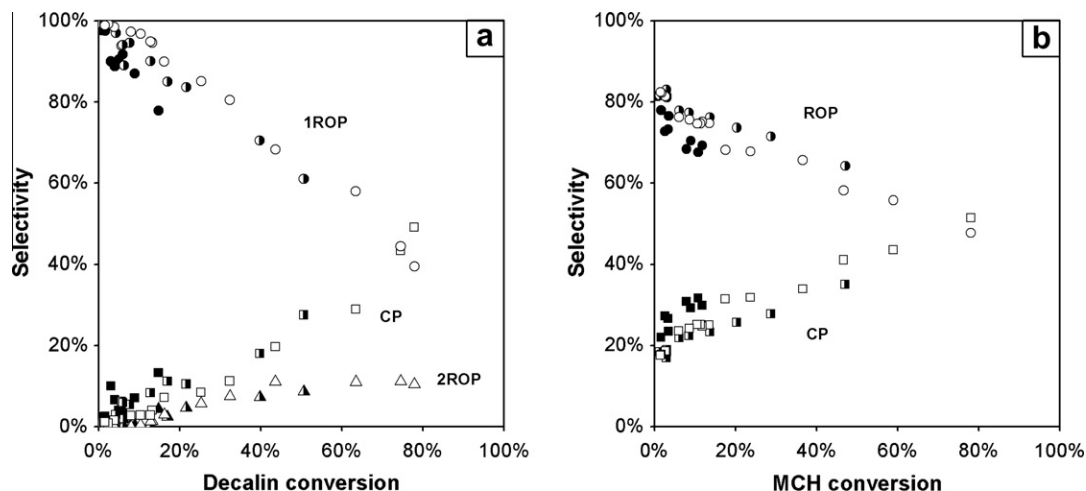
Fig. 12. Product selectivities obtained with the yIr/AW0 catalysts as a function of: (a) decalin and (b) MCH conversion (filled symbols: $y = 0.6$; half-filled symbols: $y = 1.2$; open symbols: $y = 1.8$).

conversion, essentially the same selectivities are obtained for the three catalysts. This suggests that the Ir loading has a minor influence on the product selectivity of both naphthenic molecules. For low decalin conversion, the selectivity for one-ring opening was around 100% and decreased with increasing conversion. CP selectivity was low (*ca.* 0%) for low conversion and increased with conversion. The high 1ROP selectivity observed at low decalin conversions indicates that ring opening products are primary in nature and typical of direct ring opening. Similar results have been reported by McVicker et al. [16] for the conversion of decalin over Ir/Al$_2$O$_3$ catalysts containing 0.9 wt% Ir. The decrease in 1ROP selectivity with increasing conversion can be attributed to cracking and second-ring-opening of 1ROPs. Fig. 12a also shows that 2ROP selectivity slightly increases with conversion up to a maximum of *ca.* 10% for the 1.8Ir/AW0 catalyst. Negligible amounts of aromatic compounds (e.g., tetralin) were detected.

For the MCH ring-opening reaction, in variance with the results reported for decalin, ROP and CP selectivities extrapolate, respectively, to 80% and 20% for zero conversion (instead of 100% and 0%). Thus, cracking products are partially primary in nature. Similar findings were reported by Lecarpentier et al. [13] for the ring opening of MCH over Ir/ZrO$_2$–SiO$_2$ catalysts.

Analysis of the products indicated that this could not be solely explained by the dealkylation of MCH and that a second breaking of the C–C bond appears to occur without desorption of methyl-hexane intermediates (MHx), leading to the formation of 2 and 3 methylpentanes, as well as of methane. Fig. 13 depicts the molar selectivities of the C$_{10}$H$_{20}$ 1ROPs, within the ring-opening group of products, obtained for the yIr/AW0 catalysts, as a function of decalin conversion (Fig. 13a) and the corresponding C$_7$H$_{14}$ ROPs selectivity as a function of MCH conversion (Fig. 13b). For the decalin reaction, methyl-propylcyclohexanes (MPCH) and diethylcyclohexanes (DECH) were the major products formed. It should be noted that, over these catalysts, MPCH consisted essentially of 1-methyl-2-propylcyclohexane (shown below in scheme 4), whereas over monofunctional acid catalysts, the largest fraction of MPCH corresponds to more ramified methyl-propylcyclohexanes (e.g., methyl-isopropylcyclohexane). Relatively high amounts (*ca.* 10–20%) of *n*-butylcyclohexane (BCH) and products with three or more alkyl ramifications (Others) were also detected. Analysis of the internal distribution of ROPs, for the MCH reaction, shows that 3-methylhexane (3MHx) is the most abundant compound followed by 2-methylhexane (MHx). Smaller amounts of *n*-heptane (Hp) were also detected.
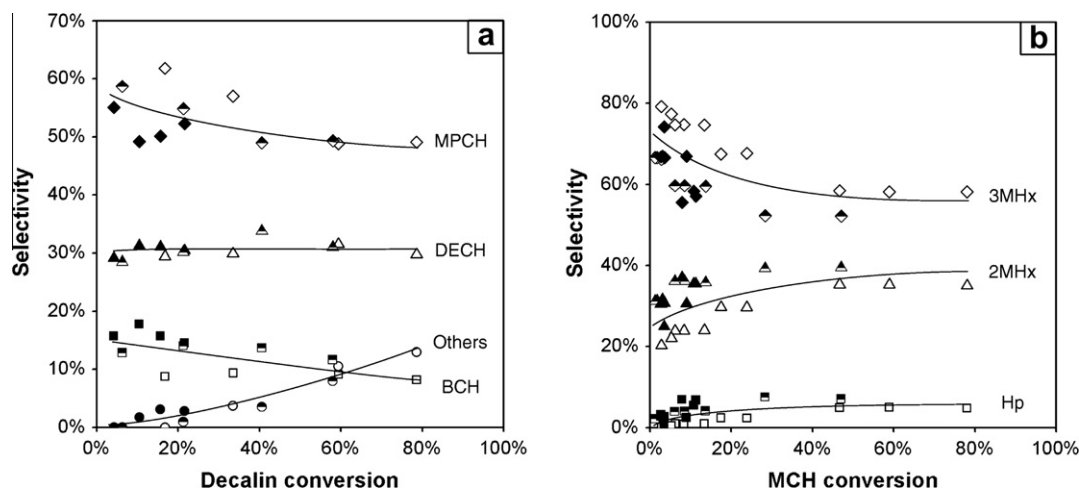

Fig. 13. Molar selectivities of: (a) C$_{10}$H$_{20}$ 1ROPs and (b) C$_7$H$_{14}$ ROPs, within the one-ring opening group of products, obtained with the yIr/AW0 catalysts, as a function of decalin and MCH conversion (filled symbols: $y = 0.6$; half-filled symbols: $y = 1.2$; open symbols: $y = 1.8$).

4. Discussion

4.1. Reaction network

Scheme 1 (a and b) depicts the proposed reaction network for the ring opening reaction of decalin and MCH, respectively.

The results obtained for the yIr/AW0 solids illustrate the ability of Ir to open directly a six-carbon-atom ring. Thus, a direct path for ring opening (r_{do}) must be considered in the proposed reaction network. It has been shown for the AWx solids that ring contraction reaction precedes that of ring opening. Such an indirect path is illustrated by two consecutive reactions: ring contraction reaction (r_{rcont}) followed by indirect ring opening (r_{io}). A second ring-opening step (r_{2ro}) was also considered for decalin, as it was observed that some catalysts yield non-negligible amounts of paraffins. In the proposed reaction network, three cracking pathways were considered: cracking of ROPs (r_{crack1}), cracking of RCPs (r_{crack2}), and cracking of 2ROPs (r_{crack3}). The direct cracking of MCH (r_{crack0}) was considered over monofunctional metal catalysts since, contrary to decalin, MCH can react by cleavage of an exocyclic bond to form methane and a cycloalkane. The proposed reaction network differs from that reported in [26] by the cracking step of ring contraction products, the second ring opening and the cracking of the 2ROPs.

4.2. Monofunctional acid catalysts

As noted earlier, analyses of the 1ROPs internal distribution (Fig. 9a) for the ring opening of decalin shows that ethyl-dimethyl-cyclohexanes (EDMCH) were the most abundant compounds followed by methyl-propylcyclohexanes (MPCH), butylcyclohexanes (BCH), pentylcyclopentanes (C5CP), and "Others" (products with three or more alkyl groups, except EDMCH).

Assuming that ring contraction precedes ring opening and that over purely acid catalysts, the ring opening mechanism proceeds via β-scission the presence of EDMCH and MPCH can be explained by ring opening of ring-contracted products, such as trimethyl-bicycloheptanes (Scheme 2) and methyl-bicyclononanes

(Scheme 3), respectively. The presence of such ring-contracted products has been authenticated by GC–MS and GC × GC analyses (not shown). In addition, they have also been observed by Kubicka et al. [28] and Santikunaporn et al. [29] for the ring opening of decalin over zeolites. Iso-butylcyclohexane can be formed as a secondary product by indirect opening of methyl-bicyclononanes [29]. It should be noted that one cannot exclude the formation of n-butyl-cyclohexane by direct ring opening of decalin (protolytic cracking mechanism) [28,33,69]. However, the results in Fig. 8, showing a near 100% RCP selectivity for low conversion, point to a minor contribution of this pathway.

Analysis of the internal distribution of ROPs, for the MCH reaction (Fig. 9b), shows that methylhexanes (2MHx and 3MHx) are the most abundant compounds followed by dimethylpentanes (23DMP and 24DMP) and heptane (Hp) in comparable amounts. The presence of 23DMP and 24DMP indicates that ring contraction precedes ring opening, since these compounds cannot be formed by direct ring opening of MCH. The presence of n-heptane can be explained by direct ring opening via β-scission of the methylcyclo-hexane carbenium ion, as suggested by Cerqueira et al. [4] for the transformation of MCH over zeolites.

4.3. Monofunctional metal catalysts

As shown in Fig. 13, the most abundant products of decalin conversion over monofunctional metal catalysts are MPCH and DECH. The formation of these compounds can be readily explained by direct ring opening. Their occurrence in a 2:1 ratio at low conversion is consistent with the dicarbene mechanism [8,16,71], which involves selective cleavage of non-substituted C–C bond (Scheme 4). However, the formation of BCH (cleavage of decalin C–C bonds at substituted positions) is not in line with this mechanism [16,71]. Its presence can be accounted for by a "partially selective" mechanism (via a metallocyclobutane intermediate) (Scheme 5), competing with the dicarbene mechanism. Such a mechanism has been proposed by Gault [8] to explain the results observed for the ring opening of methylcyclopentane over low dispersed Pt/Al$_2$O$_3$ catalysts and more recently by Do et al. [6] in the case of the direct ring
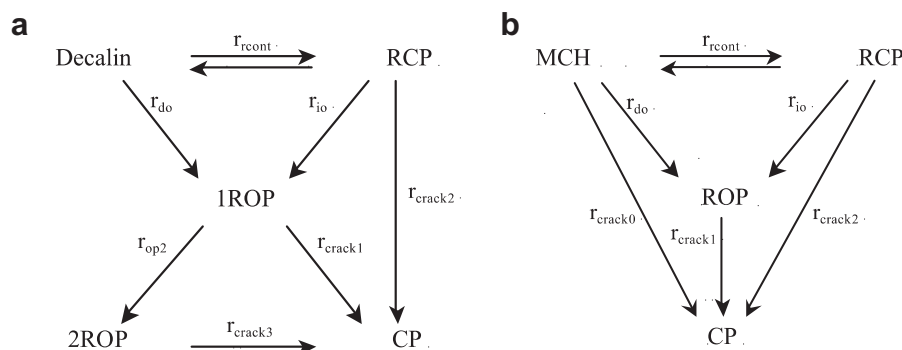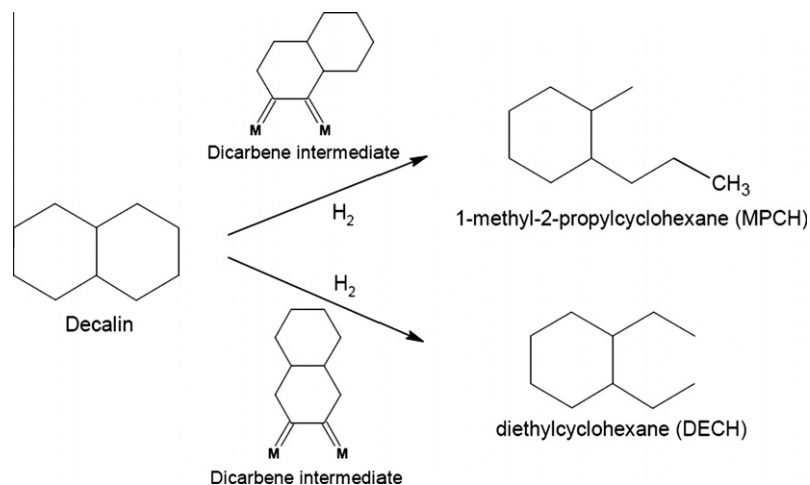

**Scheme 1.** General reaction scheme for the ring-opening reaction of: (a) decalin and (b) MCH.
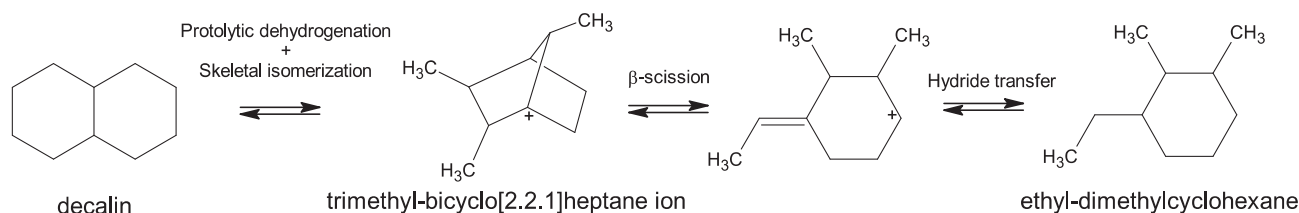
Scheme 2. Formation of EDMCH by β-scission of a trimethyl-bicyclo[2.2.1]heptane intermediate.
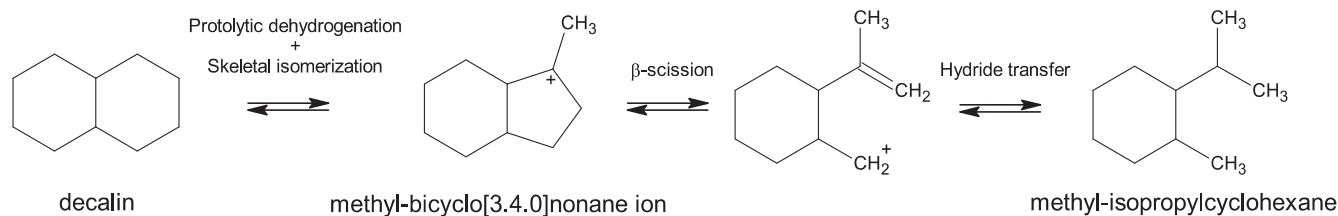
Scheme 3. Formation of MPCH by β-scission of a methyl-bicyclo[3.4.0]nonane intermediate (adapted from [28]).

Scheme 4. Reaction pathway for the selective breaking of a non-substituted carbon–carbon bond of decalin over iridium, via the dicarbene mechanism [35].
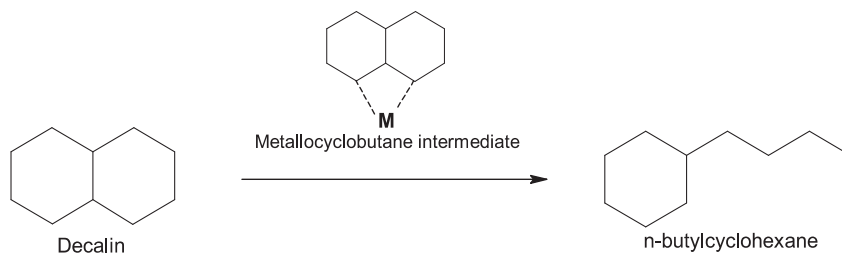
Scheme 5. Formation of butylcyclohexane from decalin via the metallocyclobutane mechanism.

opening of 1,3-dimethylcyclohexane and 1,2-dimethylcyclohexane over Ir/Al$_2$O$_3$ catalysts. Similarly, for the MCH reaction [16], the formation of *n*-heptane (cleavage of substituted C–C bonds) is consistent with ring opening via a metallocyclobutane mechanism. Note that the minor formation of the products noted as "Others" (Fig. 13) cannot be explained by direct ring opening. The presence of such products can be tentatively explained by the reported ability of iridium to promote isomerization [71–73].

4.4. Kinetic modeling – correlation between surface structure, acidity and catalytic performance

For kinetic modeling (see Supplementary materials), all the reactions shown in Scheme 1 were considered to be first order. Initial rates, determined as $r_i^\circ = k_i^\circ \cdot P^\circ$, where k_i° is the rate constant at 523 K, were calculated using the reference conditions ($P = 1$ bar). For the optimization of rate constants (k_i) and activation energies (Ea_i), the experimental data were treated as a function of the contact time and the reaction temperature. The reaction network has been used to model the performances obtained with various catalysts. A very good agreement was obtained between the calculated weight fractions and experimental results.
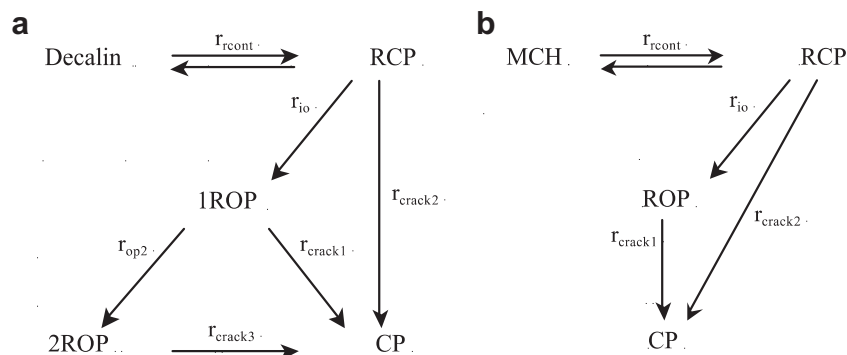
4.4.1. Monofunctional acid catalysts (AWx): influence of W surface densities

As noted earlier (Fig. 8), for these solids, ring-opening products were secondary in nature. Direct ring-opening path (r_{do}°) was thus deleted from the original general reaction network (Scheme 1). The resulting reaction networks are presented in Scheme 6.

For the decalin reaction, cracking of ring-opened products (crack 1) was observed, whereas this pathway was minor for the MCH reaction as a result of the low yield of 1ROP.

Table 3 and Table 4 report the initial rates and activation energies calculated for the decalin and MCH reaction, respectively, over the active solids (AW2.9, AW4.1, and AW5.3). The activation energies obtained for a given pathway appear to be little affected by the W surface density, suggesting a similar nature of the active sites (i.e., Brønsted acid sites of similar strength). In addition, the activation energies for ring contraction of decalin (*ca.* 80 kJ mol^{-1}) and MCH (*ca.* 95 kJ mol^{-1}) are relatively close and can be attributed, for both molecules, to the contraction of a C$_6$ ring via an acid mechanism.

Fig. 14 shows the evolution of the initial rates for ring contraction (r_{rcont}°), indirect ring opening (r_{io}°) and cracking of mono-naphthenes (r_{crack1}° for decalin and r_{crack2}° for MCH) calculated for

Scheme 6. Schematic reaction used to determine the kinetic parameters from the experimental data for the monofunctional acid catalysts. (a) Decalin and (b) MCH.

Table 3
Initial rates for the decalin reaction at 523 K and activation energies expressed respectively in mol h^{-1} kg^{-1} and kJ mol^{-1} obtained with AWx catalysts (x in at. W/nm^2).

x	r°_{rcont}	Ea$_{cont}$	r°_{io}	Ea$_{io}$	r°_{crack1}	Ea$_{crack1}$	r°_{crack2}	Ea$_{crack2}$	r°_{2ro}	Ea$_{2ro}$	r°_{crack3}	Ea$_{crack3}$
2.9	0.20	85	1.94	48	1.50	50	0.25	66	0.09	67	0.46	89
4.1	0.40	77	3.55	46	2.39	47	0.35	67	0.13	62	0.70	85
5.3	0.44	78	3.59	48	2.67	48	0.47	64	0.13	62	0.72	83

Table 4
Initial rates for the MCH reaction at 523 K and activation energies expressed respectively in mol h^{-1} kg^{-1} and kJ mol^{-1} obtained with AWx catalysts (x in at. W/nm^2).

x	r°_{rcont}	Ea$_{cont}$	r°_{io}	Ea$_{io}$	r°_{crack2}	Ea$_{crack2}$
2.9	0.09	92	0.32	56	0.06	97
4.1	0.30	97	0.88	55	0.12	100
5.3	0.32	93	0.85	51	0.11	98

the AWx as a function of W surface density. In agreement with earlier results (Fig. 7), negligible ring contraction activity (r_{rcont}) was detected for W surface densities ⩽1.4 at. W/nm^2, which is consistent with the absence of relatively strong Brønsted acid sites in these solids. For higher W surface densities, r_{rcont} increases with W surface density, reflecting the concomitant increase in the abundance of relatively strong Brønsted acid sites (Fig. 5a). This relationship is clearly illustrated in Fig. 15, which shows the initial ring contraction rate (r_{rcont}) calculated for a reaction temperature

of 523 K as a function of the area of the infrared band at 2172 cm^{-1} attributed to the interaction of CO with relatively strong Brønsted acid sites [63]. A steady increase in the ring contraction rate for both decalin and MCH reactions with the area of infrared band at 2172 cm^{-1} was obtained, whereas no such relationship was evidenced with the bands associated with Lewis acid sites. These results are consistent with those reported by Lecarpentier et al. [13], for MCH reaction over tungstated zirconia catalysts. The results in Fig. 14 also show that, for a given W surface density, the r°_{rcont} is similar for both naphthenes. However, the initial rate observed for indirect ring opening of decalin is higher than that of MCH. This can be tentatively attributed to higher strains of ring-contracted bicyclonaphthenes when compared to cyclopentanes [70] and is in line with the lower activation energy obtained for the indirect ring opening of decalin. Higher indirect ring-opening rate of decalin is also consistent with the reported increase in indirect ring opening rate with the number of tertiary carbons in the molecule [74].
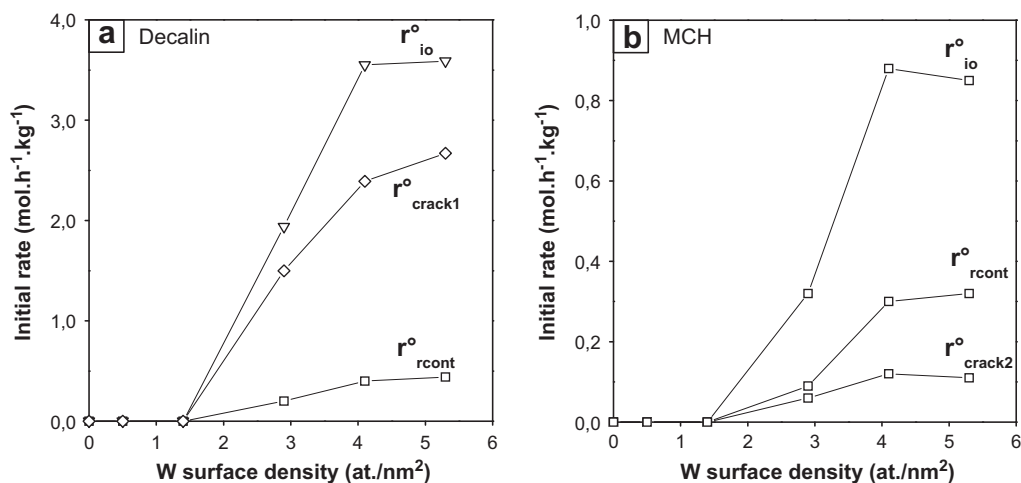

Fig. 14. Initial rates for ring contraction, indirect ring opening, and cracking obtained with the AWx catalysts as a function of W surface density. (a) decalin: r°_{rcont} (□), r°_{io} (∇), r°_{crack1} (○); (b) MCH: r°_{rcont} (□), r°_{io} (∇), r°_{crack2} (○).
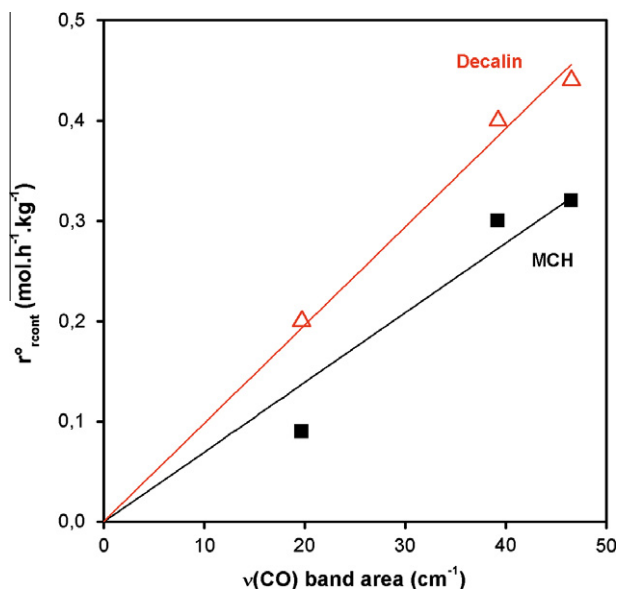
Fig. 15. Initial ring contraction rate (r_{rcont}°) at 523 K for AWx catalysts as a function of the areas of the infrared CO vibration band at 2172 cm^{-1}.

4.4.2. Monofunctional metal catalysts (yIr/AW0): influence of Ir content

As noted previously (Fig. 12), negligible activity for ring contraction was observed over these catalysts. Hence, the indirect ring-opening (r_{io}°) pathway via ring contraction of MCH was not considered in the modeling of the results. The reaction network was reduced to the following reaction network (Scheme 7).

Table 5 and 6 report the calculated direct ring opening initial rates and activation energies for the monofunctional metal catalysts obtained for the decalin and MCH reactions, respectively. The results show that, for both molecules, within the range of Ir loadings examined, Ir content seems to have no significant effect on the activation energy of a given pathway. Table 5 and 6 also indicate that similar activation energies for direct ring opening of both molecules (ca. 150 kJ mol^{-1}) were obtained. The calculated values are typical of those reported for direct ring opening via
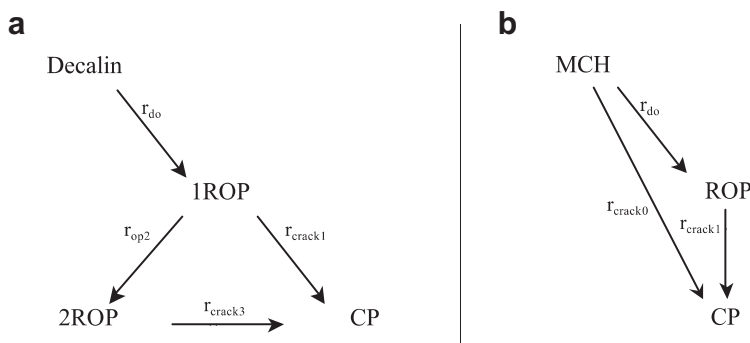
Table 6
Initial rates for the MCH reaction at 523 K and activation energies expressed respectively in mol h^{-1} kg^{-1} and kJ mol^{-1} obtained with the yIr/AW0 catalysts (y in wt.%).

y	Dispersion (%)	r_{do}°	Ea$_{do}$	r_{crack1}°	Ea$_{crack1}$	r_{crack0}°	Ea$_{crack0}$
0.6	55	0.016	158	0.032	167	0.003	184
1.2	46	0.063	155	0.085	159	0.006	176
1.8	40	0.231	152	0.201	152	0.042	167

the dicarbene mechanism [6]. This is consistent with the results described above indicating that the dicarbene mechanism is the predominant pathway for direct ring opening of decalin and MCH probe molecules.

Fig. 16 shows the evolution of the initial rates for direct ring opening (r_{do}°) and cracking of ring-opened products (r_{crack1}°), calculated for the yIr/AW0 catalysts as a function of Ir loading, for both naphthenic molecules. It is clear that, for both reactions, the initial rate of each reaction step increases with iridium content. The same tendency was observed for the remaining pathways. Similar findings were obtained when the initial rates were plotted as a function of Ir surface atoms (titrated by H$_2$ chemisorption) (Fig. 17). However, the evolution is not linear with intercept at the origin, suggesting an apparent structure sensitivity of the reaction. This is clearly illustrated in Fig. 18, which depicts the turnover frequency, TOF (expressed as initial rate r_{do}° per surface Ir atom), as a function of Ir particle size. The results show that, for both molecules, the TOF increases with increasing particle size. This is in agreement with the results of Walter et al. [22] for ring opening of MCH over Ir/Al$_2$O$_3$ catalysts and those reported by Angel et al. [75] and Fuentes et al. [7], for ring opening of methylcyclopentane and cyclohexane, respectively, over Rh/Al$_2$O$_3$ catalysts [75]. Interestingly, in the case of the related Rh system [75], the most significant variations in the TOF for methylcyclopentane conversion were observed for intermediate Ir dispersion range (between 30% and 50%). This is consistent with the results of the present study and can be interpreted, as proposed by the authors for the Rh system, in terms of changes in the surface structure of Ir particles occurring in this dispersion range. It should be noted that within the range of dispersion examined, no change in product selectivity was observed (Fig. 12 and Fig. 13).

Scheme 7. Schematic reaction used to determine the kinetic parameters from the experimental data for monofunctional metal catalysts. (a) Decalin and (b) MCH.

Table 5
Initial rates for the decalin reaction at 523 K and activation energies expressed respectively in mol h^{-1} kg^{-1} and kJ mol^{-1} obtained with the yIr/AW0 catalysts (y in wt.%).

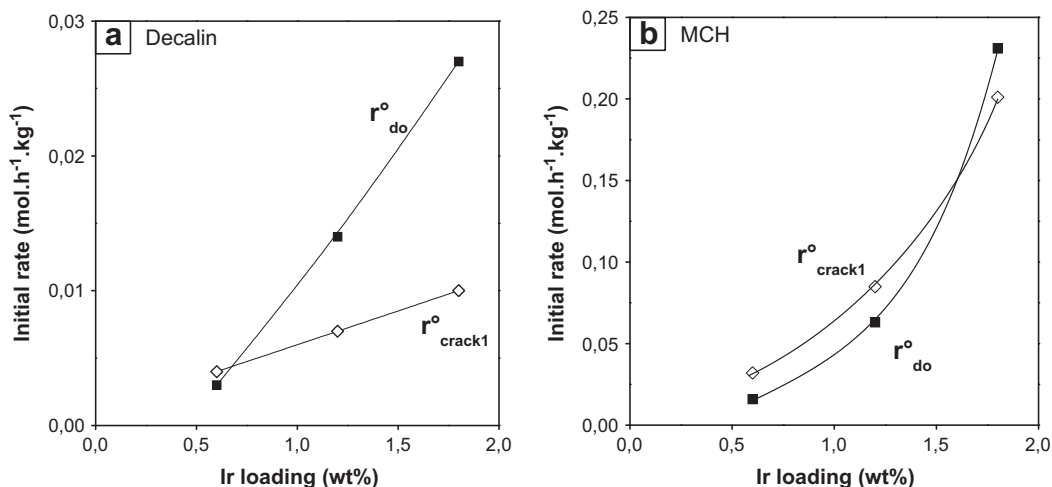| y	Dispersion (%)	r_{do}°	Ea$_{do}$	r_{crack1}°	Ea$_{crack1}$	r_{2ro}°	Ea$_{2ro}$	r_{crack3}°	Ea$_{crack3}$
0.6	55	0.003	150	0.004	167	0.004	142	0.006	167
1.2	46	0.014	146	0.007	159	0.008	138	0.013	163
1.8	40	0.027	142	0.010	159	0.014	138	0.018	163

Fig. 16. Initial rates for direct ring opening (r°_{do}) and cracking of ring opening products (r°_{crack1}) for the yIr/AW0 catalysts as a function of Ir loading. (a) Decalin and (b) MCH.
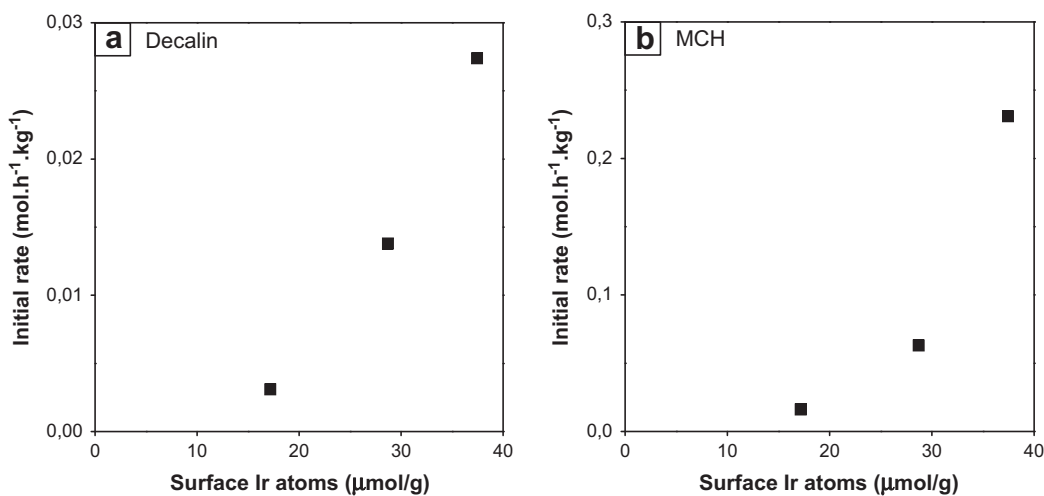

Fig. 17. Initial rate of direct ring opening (r°_{do}) at 523 K for yIr/AW0 catalysts as a function of the surface iridium atoms titrated by H_2 chemisorption. (a) Decalin and (b) MCH.
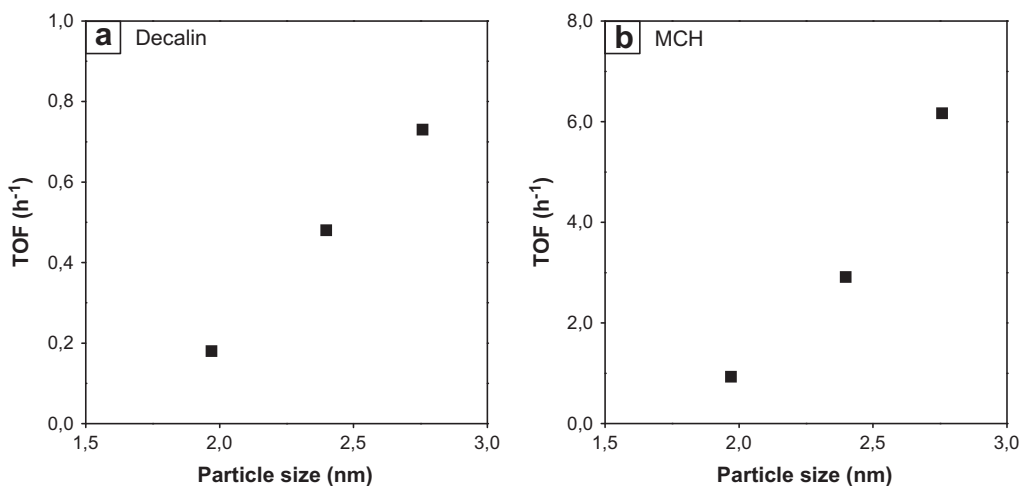

Fig. 18. Turnover frequencies (TOF) as a function of Ir particle size for direct ring-opening reaction of decalin and MCH. (a) Decalin and (b) MCH.

It should be noted that the results reported in the present study were acquired under S-free conditions. The extreme sensitivity of Ir to S (ppb levels) is well documented and is a major issue in oil refining [76–79]. In commercial practice, when Ir catalysts are used (e.g., in naphtha reforming), suitable guard beds prevent S from reaching the reactor. Thus, in principle, the sulfur content in the

feed can be extensively reduced before contact with the catalysts. However, although the topic is outside the scope of this work, a systematic study of its influence on the catalytic performance is of obvious interest.

4.5. Evaluation of possible improvement of the cetane number on decalin conversion

An assessment of possible improvement of the cetane number following ring opening was made for decalin by comparing the CN of decalin (CN = 36 [35]) with that of the most abundant 1ROPs formed. The CN of representative products resulting from opening of the first decalin ring are presented in Table 7. The internal distribution of $C_{10}H_{20}$ one-ring-opening products, over monofunctional acid catalysts (Fig. 9a), showed that ethyl-dimethylcyclohexanes (EDMCH) were the most abundant compounds followed by methyl-propylcyclohexanes (MPCH), iso-butylcyclohexanes (BCH), pentylcyclopentanes (C5CP), and "Others" (products, other than EDMCH, with three or more alkyl groups).

As shown in Table 7, EDMCH (CN = 30), MPCH (CN = 24) and BCH (CN = 36) exhibit a lower or equal CN than that of decalin (CN = 36) whereas the CN for the products C5CP and "Others" range between 15 and 29. Moreover, over these catalysts, a very high cracking selectivity was observed. This strongly suggests that no CN improvement can be obtained for the ring opening of decalin over monofunctional acid catalysts. These observations are in agreement with the predictions of cetane number improvement reported by Santana et al. [35], for acid-catalyzed ring opening of decalin.

In the case of monofunctional metal catalysts, the major products obtained were MPCH (1-methyl-2-propylcyclohexane) and DECH (cleavage of the C–C bonds at non-substituted positions), which exhibit higher cetane number than that of decalin (CN = 39). Note that the 1ROP with the highest CN (*n*-butylcyclohexane; CN = 47), formed via cleavage at substituted positions, was detected with *ca.* 10% selectivity at high conversion. In addition, *ca.* 12% of selectivity at high conversion was observed over

the monofunctional metal catalysts for 2ROPs, for which the CN can reach 77. This clearly indicates that monofunctional metal solids are better suited for the LCO upgrading than monofunctional acid catalysts. With respect to the performance of bifunctional systems, to date few studies have examined the potential improvement of cetane number based on the nature of the most abundant ring-opening products of decalin over these catalysts. Santikunaporn et al. [29] noted that over bifunctional Pt/HY catalysts, the products formed do not exhibit cetane numbers significantly higher than those of the saturated aromatics. This is consistent with the study of Santana et al. [35], which shows that only preferential cleavage at substituted C–C bonds can yield products with CN substantially higher than that of the decalin feed.
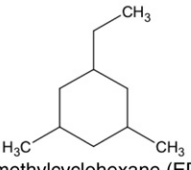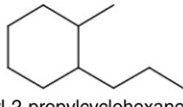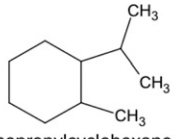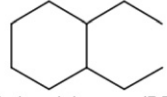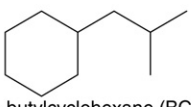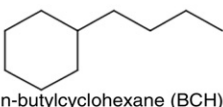
5. Conclusions

The activity and selectivity of monofunctional acid (WO_3/Al_2O_3) and metal catalysts (Ir/Al_2O_3) for ring opening reaction of decalin and methylcyclohexane (MCH) were examined.

For both molecules, the activity of monofunctional acid catalysts was only observed for W surface density higher than 1.4 at. W/nm^2, which is consistent with the development of relatively strong Brønsted acid sites. For these catalysts, ring contraction product (RCP) selectivity was high at low conversion and decreased with increasing conversion, indicating that ring contraction is the first step for ring opening of decalin and MCH. The decrease in RCP selectivity was less pronounced for the MCH reaction when compared to that of decalin, suggesting that the RCPs formed during the MCH reaction are less reactive than those of decalin. Naphthenes ring opening occurs according to an acid mechanism, which involves protolytic dehydrogenation, skeletal isomerization, β-scission, and hydride transfer. For the active catalysts, the low selectivity for one-ring opening and the low CN of the 1ROP formed suggest that these are not suitable catalysts for the upgrading of LCO.

The performance of monofunctional metal catalysts *y*Ir/AW0 was also compared for both naphthenic molecules. Conversion

Table 7
Major products and respective cetane number obtained for the ring opening of decalin, over monofunctional acid and metal catalysts [35].

Monofunctional acid (AWx)	Monofunctional metal (*y*Ir/AW0)
ethyldimethylcyclohexane (EDMCH) **CN=30**	1-methyl-2-propylcyclohexane (MPCH) **CN=39**
methyl-isopropylcyclohexane (MPCH) **CN=24**	diethyl-cyclohexane (DECH) **CN=39**
iso-butylcyclohexane (BCH) **CN=36**	n-butylcyclohexane (BCH) **CN=47**

was relatively low for the lowest Ir loading and increases significantly with increasing iridium content. Ir loading has a minor influence on the product selectivity for both naphthenic molecules. For low conversion, the results for monofunctional metal catalysts showed that ROP selectivity is high and decreases with increasing conversion.

The internal distribution of $C_{10}H_{20}$ one-ring-opening products evidenced that, over Ir/Al$_2$O$_3$, hydrogenolysis via the dicarbene mechanism is the preferred path to ring open both naphthenes. However, a competitive "partially selective" mechanism (via a metallocyclobutane intermediate), leading to the formation of high CN products, is also operative. The CN and the ring opening products selectivity (1ROP and 2ROP) obtained from ring opening over monofunctional metal catalysts suggest that these catalysts are better suited for the LCO upgrading than monofunctional acid catalysts.

Appendix A. Supplementary material

Supplementary data associated with this article can be found, in the online version, at doi:10.1016/j.jcat.2011.10.014.

References

[1] H. Belatel, H. Al-Kandari, F. Al-Khorafi, A. Katrib, F. Garin, Appl. Catal. A 275 (2004) 141.
[2] V. Calemma, A. Carati, C. Flego, R. Giardino, R. Millini, Abstr. Pap. Am. Chem. Soc. 229 (2005) 51.
[3] P. Castaño, A.G. Gayubo, B. Pawelec, J.L.G. Fierro, J.M. Arandes, Chem. Eng. J. 140 (2008) 287.
[4] H.S. Cerqueira, P.C. Mihindou-Koumba, P. Magnoux, M. Guisnet, Ind. Eng. Chem. Res. 40 (2001) 1032.
[5] A. Corma, F. Mocholi, V. Orchilles, G.S. Koermer, R.J. Madon, Appl. Catal. 67 (1991) 307.
[6] P.T. Do, W.E. Alvarez, D.E. Resasco, J. Catal. 238 (2006) 477.
[7] S. Fuentes, F. Figueras, J. Catal. 61 (1980) 443.
[8] F.G. Gault, Adv. Catal. 30 (1981) 1.
[9] H. Glassl, K. Hayek, R. Kramer, J. Catal. 68 (1981) 397.
[10] S.L. Gonzalez-Cortes, S. Dorkjampa, P.T. Do, Z. Li, J.M. Ramallo-Lopez, F.G. Requejo, Chem. Eng. J. 139 (2008) 147.
[11] R. Kramer, H. Zuegg, J. Catal. 80 (1983) 446.
[12] R. Kramer, H. Zuegg, J. Catal. 85 (1984) 530.
[13] S. Lecarpentier, J. Van Gestel, K. Thomas, J.-P. Gilson, M. Houalla, J. Catal. 254 (2008) 49.
[14] F. Locatelli, D. Uzio, G. Niccolai, J.M. Basset, J.P. Candy, Catal. Commun. 4 (2003) 189.
[15] G. Maire, G. Plouidy, J.C. Prudhomme, F.G. Gault, J. Catal. 4 (1965) 556.
[16] G.B. McVicker, M. Daage, M.S. Touvelle, C.W. Hudson, D.P. Klein, W.C.J. Baird, B.R. Cook, J.G. Chen, S. Hantzer, D.E.W. Vaughan, E.S. Ellis, O.C. Feeley, J. Catal. 210 (2002) 137.
[17] G.B. McVicker, O.C. Feeley, J.J. Ziemiak, D.E. Vaughan, K.C. Strohmaier, W.R. Kliewer, D.P. Leta, J. Phys. Chem. B 109 (2005) 2222.
[18] G. Moretti, W.M.H. Sachtler, J. Catal. 116 (1989) 350.
[19] A. Raichle, Y. Traa, F. Fuder, M. Rupp, J. Weitkamp, Angew. Chem. Int. Ed. 40 (2001) 1243.
[20] G. Rodriguez-Gattorno, L.O. Aleman-Vazquez, X. Angeles-Franco, J.L. Cano-Dominguez, R. Villagomez-Ibarra, Energy Fuels 21 (2007) 1122.
[21] T. Sugii, Y. Kamiya, T. Okuhara, Appl. Catal. A 312 (2006) 45.
[22] C.G. Walter, B. Coq, F. Figuéras, Appl. Catal. A 133 (1995) 95.
[23] Z. Wang, A. Nelson, Catal. Lett. 123 (2008) 226.
[24] Y. Zhuang, A. Frennet, Appl. Catal. A 134 (1996) 37.
[25] B.H. Cooper, B.B.L. Donnis, Appl. Catal. A 137 (1996) 203.
[26] D. Kubicka, N. Kumar, P. Mäki-Arvela, M. Tiitta, V. Niemi, H. Karhu, T. Salmi, D.Y. Murzin, J. Catal. 227 (2004) 313.
[27] D. Kubicka, T. Salmi, M. Tiitta, D.Y. Murzin, Fuel 88 (2009) 366.
[28] D. Kubicka, N. Kumar, P. Mäki-Arvela, M. Tiitta, V. Niemi, T. Salmi, D.Y. Murzin, J. Catal. 222 (2004) 65.
[29] M. Santikunaporn, J.E. Herrera, S. Jongpatiwut, D.E. Resasco, W.E. Alvarez, E.L. Sughrue, J. Catal. 228 (2004) 100.
[30] K.C. Mouli, V. Sundaramurthy, A.K. Dalai, Z. Ring, Appl. Catal. A 321 (2007) 17.
[31] K.C. Mouli, V. Sundaramurthy, A.K. Dalai, J. Mol. Catal. A: Chem. 304 (2009) 77.
[32] D.Y. Murzin, D. Kubicka, I.L. Simakova, N. Kumar, A. Lazuen, P. Maki-Arvela, M. Tiitta, T. Salmi, Pet. Chem. 49 (2009) 90.
[33] A. Corma, V. Gonzalez-Alfaro, A.V. Orchilles, J. Catal. 200 (2001) 34.
[34] S. Dokjampa, T. Rirksomboon, S. Osuwan, S. Jongpatiwut, D.E. Resasco, Catal. Today 123 (2007) 218.
[35] R.C. Santana, P.T. Do, M. Santikunaporn, W.E. Alvarez, J.D. Taylor, E.L. Sughrue, D.E. Resasco, Fuel 85 (2006) 643.
[36] C. Flego, N. Gigantiello, W.O. Parker Jr, V. Calemma, J. Chromatogr. A 1216 (2009) 2891.
[37] A. Slagtern, I.M. Dahl, K.J. Jens, T. Myrstad, Appl. Catal. A 375 (2010) 213.
[38] C. Berger, A. Raichle, R.A. Rakoczy, Y. Traa, J. Weitkamp, Micropor. Mesopor. Mater. 59 (2003) 1.
[39] Z. Paál, P. Tetenyi, Nature 267 (1977) 234.
[40] P. Samoila, M. Boutzeloit, C. Especel, F. Epron, P. Marécot, Appl. Catal. A 369 (2009) 104.
[41] B. Coq, E. Crabb, F. Figuéras, J. Mol. Catal. A: Chem. 96 (1995) 35.
[42] H. Schulz, J. Weitkemp, H. Eberth, in: J.W. Hightower (Ed.), Proc. 5th ICC, North-Holland, Amsterdam, 1973, p. 1229.
[43] G. Onyestyak, G. Pál-Borbély, H.K. Beyer, Appl. Catal. A 229 (2002) 65.
[44] W.C. Baird, D.P. Klein, J.G. Chen, G.B. McVicker, US Patent 6683020, 2004 (to Exxon-Mobil).
[45] S. Lecarpentier, J. Van Gestel, J.-P. Dath, C. Collet, J.-P. Gilson, WO Patent Application 2007/006924, 2007 (to Total-France).
[46] M.A. Arribas, P. Concepción, A. Martínez, Appl. Catal. A 267 (2004) 111.
[47] T.N. Vu, J. van Gestel, J.-P. Gilson, C. Collet, J.-P. Dath, J.C. Duchet, J. Catal. 231 (2005) 453.
[48] J.-W. Park, K. Thomas, J. van Gestel, J.-P. Gilson, C. Collet, J.-P. Dath, M. Houalla, Appl. Catal. A 388 (2010) 37.
[49] D.S. Cunha, G.M. Cruz, Appl. Catal. A 236 (2002) 55.
[50] P.N. Da Silva, M. Guenin, C. Leclercq, R. Frety, Appl. Catal. 54 (1989) 203.
[51] T. Onfroy, G. Clet, M. Houalla, J. Phys. Chem. B (2005).
[52] S.S. Chan, I.E. Wachs, L.L. Murrell, N.C. Dispenziere, in: S. Kaliaguine, A. Mahay (Eds.), Stud. Surf. Sci. Catal., Elsevier, 1984, p. 259.
[53] I.E. Wachs, Catal. Today 27 (1996) 437.
[54] O. Cairon, T. Chevreau, J.C. Lavalley, J. Chem. Soc. Faraday Trans. 94 (1998) 3039.
[55] O. Cairon, K. Thomas, A. Chambellan, T. Chevreau, Appl. Catal. A 238 (2003) 167.
[56] L.M. Kustov, V.B. Kazanskii, S. Beran, L. Kubelkova, P. Jiru, J. Phys. Chem. 91 (1987) 5247.
[57] L. Kubelkova, S. Beran, J.A. Lercher, Zeolites 9 (1989) 539.
[58] C. Pfaff, M.J.P. Zurita, C. Scott, P. Patino, M.R. Goldwasser, J. Goldwasser, F.M. Mulcahy, M. Houalla, D.M. Hercules, Catal. Lett. 49 (1997) 13.
[59] L. Karakonstantis, C. Kordulis, A. Lycourghiotis, Langmuir 8 (1992) 1318.
[60] W.S. Millman, M. Crespin, A.C. Cirillo, S. Abdo, W.K. Hall, J. Catal. 60 (1979) 404.
[61] A.M. Turek, I.E. Wachs, E. Decanio, J. Phys. Chem. 96 (1992) 5000.
[62] C. Morterra, G. Magnacca, Catal. Today 27 (1996) 497.
[63] X. Chen, G. Clet, K. Thomas, M. Houalla, J. Catal. 273 (2010) 236.
[64] S.L. Soled, G.B. McVicker, L.L. Murrell, L.G. Sherman, N.C. Dispenziere, S.L. Hsu, D. Waldman, J. Catal. 111 (1988) 286.
[65] W.-C. Lai, C. Song, Catal. Today 31 (1996) 171.
[66] E.F. Sousa-Aguiar, C.J.A. Mota, M.L. Valle Murta, M. Pinhel da Silva, D. Forte da Silva, J. Mol. Catal. A: Chem. 104 (1996) 267.
[67] C.J. Egan, G.E. Langlois, R.J. White, J. Am. Chem. Soc. 84 (1962) 1204.
[68] D.M. Brouwer, H. Hogeveen, Recl. Trav. Chim. Pays-Bas 89 (1970) 211.
[69] H.B. Mostad, T.U. Riis, O.H. Ellestad, Appl. Catal. 63 (1990) 345.
[70] K.B. Wiberg, Angew. Chem.-Int. 25 (1986) 312.
[71] F. Weisang, F.G. Gault, J. Chem. Soc. Chem. Commun. 11 (1979) 519.
[72] D. Kubicka, N. Kumar, P. Mäki-Arvela, T. Venäläinen, M. Tiitta, T. Salmi, D.Y. Murzin, Stud. Surf. Sci. Catal. 158 (2005) 1669.
[73] F.G. Gault, V. Amirebrahimi, F. Garin, P. Parayre, F. Weisang, Bull. Soc. Chim. Belg. 88 (1979) 475.
[74] C. Marcilly, Catalyse acido-basique, Application au Raffinage et à la Pétrochimie, Editions Technip, 2003.
[75] G.D. Angel, B. Coq, R. Dutartre, F. Figuéras, J. Catal. 87 (1984) 27.
[76] J. Barbier, E. Lamy-Pitara, P. Marécot, J.P. Boitiaux, J. Cosyns, F. Verna, Adv. Catal. 37 (1990) 279.
[77] R. Frety, P.N. Da Silva, M. Guenin, Appl. Catal. 57 (1990) 99.
[78] S. Nassreddine, L. Massin, M. Aouine, C. Geantet, L. Piccolo, J. Catal. 278 (2011) 253.
[79] R.W. Rice, D.C. Keptner, Appl. Catal. A 262 (2004) 233.